Metabolomics Vol. 1, No. 2, April 2005 (© 2005)
DOI: 10.1007/s11306-005-4428-3

Characterizing the metabolic actions of natural stresses in the California red abalone, *Haliotis rufescens* using ^{1}H NMR metabolomics

E.S. Rosenblum[a,*], M.R. Viant[b], B.M. Braid[c], J.D. Moore[c], C.S. Friedman[d], and R.S. Tjeerdema[a]

[a]*Department of Environmental Toxicology, University of California, One Shields Avenue, Davis, CA, 95616, USA*
[b]*School of Biosciences, The University of Birmingham, Edgbaston, Birmingham, B15 2TT, UK*
[c]*School of Veterinary Medicine, University of California, One Shields Avenue, Davis, CA, 95616, USA*
[d]*School of Aquatic and Fishery Sciences, University of Washington, Box 355020, Seattle, WA, 98195, USA*

Received 7 December 2004; accepted 18 March 2005

Withering syndrome in California red abalone (*Haliotis rufescens*) is caused by the Rickettsiales-like prokaryote (WS-RLP) *Candidatus Xenohaliotis californiensis*. WS-RLP infection is not sufficient to cause withering syndrome, and for reasons not yet well understood additional stressors such as elevated water temperature appear to influence disease development. Using nuclear magnetic resonance (NMR) based metabolomics, we have investigated the influence of food availability, temperature, and bacterial infection, both individually and in combination, on the metabolic status of the red abalone. Food limitation caused dramatic reductions in all observed classes of foot muscle metabolites, while at the same time metabolite levels within the digestive gland were preserved or increased. We also found that food limitation in combination with elevated temperature led to greater metabolic perturbations in both tissue types than those observed under food limitation alone. WS-RLP infection and food-limitation resulted in many of the same metabolic changes within the tissues studied, although the effects of infection were less severe. We observed increased levels of homarine in the digestive gland of both food-limited and WS-RLP-infected animals, yet only observed increased homarine levels in the foot muscle of infected abalone. These results further support the recently established glucose-to-homarine ratio in foot muscle as a potential marker for differentiating WS-RLP-infected animals from those of both healthy and food limited abalone. Furthermore, we found that the NMR metabolic data correlates well with histological measurements supporting the use of the metabolomics approach for characterizing both normal and pathological events in marine species, particularly during periods of environmentally relevant stress.

KEY WORDS: withering syndrome; abalone; NMR; metabolomics; disease; homarine.

1. Introduction

Abalones are members of a large class of marine molluscs (Gastropoda). They belong to the family Haliotidae and the genus *Haliotis*, which means sea ear, referring to the flattened shape of the shell. Withering syndrome (WS) is a fatal disease that has had profound effects both on wild California abalone and their culture industry. WS has been observed in black *(Haliotis cracherodii)*, red *(Haliotis rufescens)*, pink *(H. corrugata)*, green *(H. fulgens)* and white *(H. sorenseni)* abalone (Moore *et al.*, 2002). Natural populations of Southern California abalone impacted by WS have failed to recover following fishery closures, and while the contribution of WS is unclear it appears to be significant in at least some species (Moore *et al.*, 2002). WS spread northward throughout the 1990s, and abalone with symptoms of the disease have been observed as far north as Point San Pedro (San Francisco County, CA) in 1999 (Friedman and Finley, 2003).

The causative agent of WS is the pathogen *Candidatus Xenohaliotis californiensis*, a Rickettsiales-like prokaryote (WS-RLP; Friedman *et al.*, 2000; Moore *et al.*, 2001; Friedman and Finley, 2003). Animals with signs of the disease experience metaplastic changes in the digestive gland, in which the terminal acini that secrete digestive enzymes are replaced with transport epithelia (Gardner *et al.*, 1995). It is speculated that animals showing signs of WS have lost the ability to digest food, and become dependent on stored energy (Kismohandaka *et al.*, 1993; Shields *et al.*, 1996). Researchers have confirmed that alterations in the digestive gland precede both depletion of glycogen reserves and utilization of the foot muscle as an energy source (Gardner *et al.*, 1995). This shift in metabolism eventually leads to the major sign of the syndrome, a shrunken foot, which is hypothesized to be the result of physiological starvation.

Infection with the rickettsial parasite, however, does not necessarily produce signs of the disease, and for

* To whom correspondence should be addressed.
E-mail: Esrosenblum@UCDavis.Edu

1573-3882/05/0400–0199/0

reasons not yet well understood some infected abalone do not develop WS. Possible explanations include variable pathogenicity among strains of the infectious organism and variable innate host susceptibility. Both field and laboratory studies with red abalone have shown that elevated water temperature hastens the progression of WS and increases mortality (Lafferty and Kuris, 1993; Friedman *et al*., 1997; Moore *et al*., 2000; Raimondi *et al*., 2002; Vilchis *et al*., 2005). Vilchis *et al*. (2005) described increased morbidity and mortality attributed to WS under conditions of elevated water temperature and reduced food availability, which co-occur during warm water events such as the El Niño Southern Oscillation.

These studies suggest, at least in the short term, that red abalone require a thermal stress to develop WS, and reaffirm that the presence of the WS-RLP alone is not sufficient to cause the development of WS. It is known that sub-lethal stress can play a role in the reduction of an organism's energy stores (Bayne, 1985; Rainbow and Phillips, 1993), and that the presence of multiple sublethal stressors can have additive effects, potentially making an organism more vulnerable to an additional environmental insult (Isani *et al*., 1997).

Here we have investigated the effects of elevated water temperature, reduction of food availability, and presence of WS-RLP on the metabolic profiles of the foot muscle and digestive gland of red abalone. The primary goal of the study is to achieve greater mechanistic insight into the response of different tissues to the sublethal stressors in abalone, specifically the conditions that favor the development of WS. We have addressed the hypotheses that WS-RLP infection in red abalone is metabolically equivalent to starvation and that the combined effects of thermal stress along with starvation has a more profound impact on the metabolic profiles when encountered together than those observed due to starvation alone. To achieve these objectives all stressors were applied individually and in combination. This investigation was conducted using a ^{1}H NMR metabolomics approach which measures the molecular phenotype of an organism directly, and provides an integrated ''snapshot'' of the low molecular weight metabolites that can change during the disease process (Viant *et al*., 2003). This approach facilitated our secondary goal of establishing a group of biomarkers that can be used in rapid screening between these sublethal environmental stressors.

2. Materials and methods

2.1. Animals

A total of 1500 red abalone approximately 3 cm in length were obtained from The Abalone Farm Inc., Cayucos, California. Prior to transport to the Bodega Marine Laboratory, the abalone were fed a medicated artificial diet containing 1.3% active oxytetracycline at a rate of 1% of tank biomass for 14 days, and then fed kelp (*Macrocystis pyrifera*) for 1 month (Friedman *et al*., 2003). Upon arrival they were divided into four groups of approximately 375 animals and each group was placed in a 122 L tank receiving a constant supply of aerated, flow-through, ambient (approx. 12.3°C) seawater. To ensure that no residual WS-RLP infections existed in the animals they were again fed 1.4% active OTC medicated feed at 6 g total OTC/100 lbs abalone for 21 days, and then fed kelp *ad libitum* for 16 days. Ten animals were sacrificed and both histology (Friedman *et al*., 2000) and PCR (Andree *et al*., 2000) were used to assess WS-RLP status, the results in both cases showing no infection was present (Braid *et al*., 2004). A subset of the remaining animals was then re-infected through cohabitation with known infected animals and by exposure to effluent from a header tank containing infected red abalone (Moore *et al*., 2001).

2.2. Experimental design

After co-habitation for 1 month, the WS-RLP exposed and WS-RLP free abalone were equally divided between 48 2-L containers (designated as day 0), providing six replicate containers for each of the eight treatment conditions described below (figure 1). The eight treatments consisted of each of the factors, WS-RLP exposure (exposed or unexposed), water temperature (ambient 12.3°C or heated to ca. 18°C) and food availability (fed *ad libitum* or reduced food) in the following combinations: UHF (unexposed/heated/fed), UAF (unexposed/ambi-

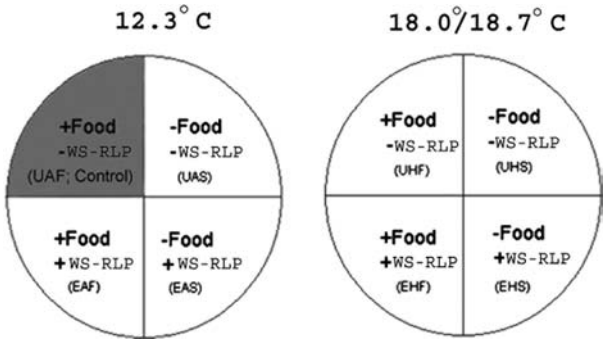

Figure 1. Experimental design involving eight treatment groups: UHF (unexposed/heated/fed), UAF (unexposed/ambient/fed; control group), UHR (unexposed/heated/reduced food), UAR (unexposed/ambient/reduced food), EHF (exposed/heated/fed), EAF (exposed/ambient/fed), EAR (exposed/ambient/reduced food) and EHR (exposed/heated/reduced food). Each treatment consisted of $n = 6$ independent tanks. Due to the high mortality rates that occurred in the EHR treatment, no animals were available for analysis. Foot muscle NMR data set consisted of 62 samples, allowing at least one sample measurement to be made on each of the six replicate tanks from the above seven treatment conditions. The digestive gland data set consists of 40 samples allowing 6 replicate measurements to be made per treatment condition except UHR which only contains 4 replicates.

ent/fed; control group), UHR (unexposed/heated/reduced food), UAR (unexposed/ambient/reduced food), EHF (exposed/heated/fed), EAF (exposed/ambient/fed), EHR (exposed/heated/reduced food), and EAR (exposed/ambient/reduced food). Mean temperatures for the heated unexposed and heated exposed groups were 18.0 and 18.7°C, respectively, and 12.3°C for both the unexposed and exposed ambient groups. Animals included in this study were subjected to the above conditions for 497 days. All fed groups were supplied kelp *ad libitum*.

Initially the food limited groups received one-quarter of the ration of the fed groups, however on sampling day 277, no body shrinkage had yet occurred and foot muscle and digestive gland glycogen levels had not appreciably decreased (Braid *et al.*, 2004). Therefore, on day 290 their kelp ratio was discontinued through sample day 497. Three abalone from each container (total of 18 abalone per treatment) were randomly selected, sacrificed, and foot muscle and digestive gland were dissected and flash frozen in liquid nitrogen. Due to the high mortality rates that occurred in the EHR treatment no animals were available for analysis. Sixty-two foot muscle samples were measured by NMR, allowing at least one sample measurement to be made on each of the six replicate tanks from the above seven treatment conditions. The digestive gland data set consists of 40 samples allowing 6 replicate measurements to be made per treatment condition except UHR which only contains four replicates. Tissues were stored at −80°C until extraction. Animals that died during the experiment were not included in the metabolic evaluation.

2.3. Histology

Tissue sections from the post-esophagus, digestive gland, foot muscle, and kidney were fixed overnight in 3.5% paraformaldehyde in phosphate-buffered saline, and then transferred to 70% ethanol. Paraffin-embedded tissue sections sections (5 μm) were deparaffinized, stained with hematoxylin and eosin, and viewed by light microscopy.

Stained sections were rated following the scales devised by Friedman *et al.* (1997) and Moore *et al.* (2000). Foot muscle atrophy: 0 = Muscle fibers comprise >90% of tissue present, 1 = 76–90%, 2 = 50–75%, 3 = <50%. Post-esophagus and digestive gland WS-RLP infection intensity: 0 = absent, 1 = 1–10 inclusions/20 × field of view, 2 = 11–100, 3 = >100. Digestive gland atrophy: 0 = connective tissue comprises <5% of tissue, 1 = 5–10%, 2 = 11–25%, 3 = >25%. Area of digestive gland occupied by transport duct, termed "metaplasia" in previous reports: 0 = transport ducts comprise <5% of tissue, 1 = 5–10%, 2 = 11–25%, 3 = >25% (Braid *et al.*, 2004).

2.4. ^1H NMR spectroscopy

Digestive gland and foot muscle samples were analyzed using ^{1}H NMR, as described previously (Viant *et al.*, 2003). Briefly, frozen samples were prepared by perchloric acid extraction, followed by lyophilization and resuspension in 0.2 M sodium phosphate buffer in D_2O with 1 mM sodium 3-(trimethylsilyl) propionate-2,2,3,3-d_4 (TMSP) NMR standard. Foot muscle extracts were analyzed at 500.11 MHz using an Avance DRX-500 spectrometer (Bruker, Fremont, CA) at 295 K using a 1D sequence with pre-saturation of the water resonance. To facilitate removal of broad resonances from high-molecular weight compounds, ^{1}H NMR spectra of digestive gland extracts were obtained using a Carr–Purcell–Meiboom–Gill spin–echo sequence. The resulting spectra were phased; baseline corrected and calibrated (TMSP peak at 0.0 ppm) using XWINNMR software (Version 3.1; Bruker). Peaks were assigned by comparison to tabulated chemical shifts (Fan, 1996; Viant *et al.*, 2003) and confirmed by 2D NMR methods, including ^{1}H–^{1}H homonuclear correlation spectroscopy (COSY), and ^{1}H–^{13}C heteronuclear single quantum coherence (HSQC). Significant differences between the metabolic profiles of the treatment groups were identified using pattern recognition methods, as described below.

2.5. Pre-processing of NMR data

The 1D NMR spectra were converted to an appropriate format for multivariate analysis using custom-written *ProMetab* software (Viant, 2003) in MATLAB (Version 6.1; The MathWorks, Natick, MA). Each NMR spectrum was divided into 1960 chemical shift bins between 0.2–10.0 ppm, corresponding to a bin width of 0.005 ppm (2.5 Hz). The residual water peak was excluded from each spectrum and the spectral area within the remaining bins formed a vector containing intensity-based descriptors of the original spectrum. Each spectrum was normalized to dry tissue weight enabling interpretation of relative metabolite levels on a dry mass basis (Viant *et al.*, 2003). All elements of the matrices were log transformed, and the columns mean-centered before multivariate analysis. Metabolite levels were calculated by integrating the appropriate chemical shift bins prior to log transformation.

2.6. Principal components analysis

Principal components analyses (PCA) of the pre-processed NMR data were conducted using the PLS_Toolbox (Version 2.1; Eigenvector Research, Manson, WA) within MATLAB. Statistical tests were performed using Number Cruncher Statistical System (2001 Edition; NCSS Statistical Software, Kaysville, UT). The classification of the heat stressed, food limited, and

diseased abalone along the PC axes were analyzed using one-way ANOVAs. Comparisons of the response of individual metabolite peak areas within the various treatment groups were conducted using one-way ANOVAs followed by Tukey–Kramer post-hoc tests. Peak areas within a treatment group were subjected to multivariate outlier tests based on the Mahalanobis distance of each point from the variable means with a T^2 alpha setting of 0.05 (NCSS).

3. Results and discussion

3.1. Metabolites in tissue extracts

Metabolites observed in red abalone foot muscle and digestive gland extracts have been previously identified and verified by 1- and 2-D NMR methods (Viant *et al.*, 2003). Representative spectra collected in the current study include amino acids (Ala, Asp, Glu, Gln, Gly, Leu, Ile, Lys, Pro, Thr, Val, Tyr, Trp, Phe, taurine), α- and β-glucose, carnitine, phosphagens, nucleotides, glycolytic products and citric acid cycle intermediates (figure 2a and b). Several metabolites remain unidentified (or unobserved) because they either exist below detection limits or have been obscured by signals from other compounds, which was particularly prevalent in the aliphatic spectral region.

3.2. NMR spectral analysis

Principal components analyses (PCA) provides a method of simultaneously comparing all the animals' entire NMR metabolic profiles and yielding simple graphical outputs where each spectrum is denoted as a single point. Close spatial proximity within a PCA scores plot denotes similar NMR spectra and thus similar metabolic phenotype. Figure 3a and b display scores plots of the entire foot muscle ($n = 62$) and digestive gland ($n = 40$) data sets used in this analysis. The first two PC axes describe 92.7% and 70.8% of the variability that exists within the foot muscle and the digestive gland data sets, respectively.

3.3. Metabolic response to food limitation

One-way ANOVAs followed by post-hoc tests conducted on the various treatment groups PC scores reveal that separation due to food reduction regardless of temperature is highly significant in both the foot muscle and digestive gland ($p < 0.0001$). Additionally, in the PCA scores plots of the foot muscle spectra we find evidence that the combination of both elevated water temperatures and food limitation after 447 days of exposure causes a more dramatic metabolic response than that observed in food limitation alone.

The shifts observed along the PC axis in the reduced food foot muscle groups at both temperatures is caused by decreases in all classes of foot muscle metabolites. This is clearly displayed in decreases observed in both the total spectral areas (table 1), giving insight into how food limitation affected all detectable metabolites, and in identified NMR peaks, which were found to change significantly (table 2). The observed reduction in foot muscle total spectral areas within the food limited treatment groups is most likely due to break down of the tissue and increased infiltration of hemolymph/water. Both histological observation of foot degeneration and tissue dry/wet mass ratios are consistent with this. While tissue dry/wet mass ratios (table 1) were not significantly different between the reduced food groups at two

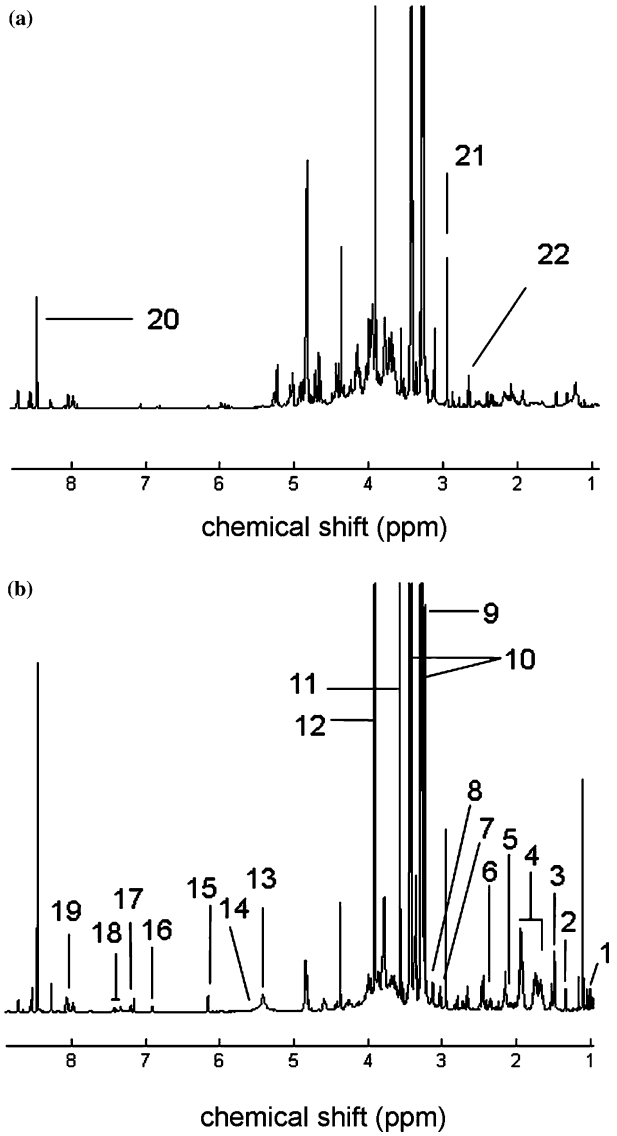

Figure 2. Representative one-dimensional ^{1}H NMR spectra of a healthy abalone (a) foot muscle and (b) digestive gland. Metabolites are: 1. Val, 2. Thr, 3. Ala, 4. phosphoarginine + Arg, 5. Gln, 6. Pro, 7. Lys, 8. acetylcholine[a], 9. carnitine, 10. taurine, 11. glycine–betaine, 12. Gly, 13. glycogen, 14. α-glucose, 15. ATP + ADP, 16. Tyr, 17. Trp, 18. Phe, 19. homarine, 20. formate, 21. dimethylglycine[a], 22. *N*-methyltaurine[a].
[a]Unconfirmed assignments.

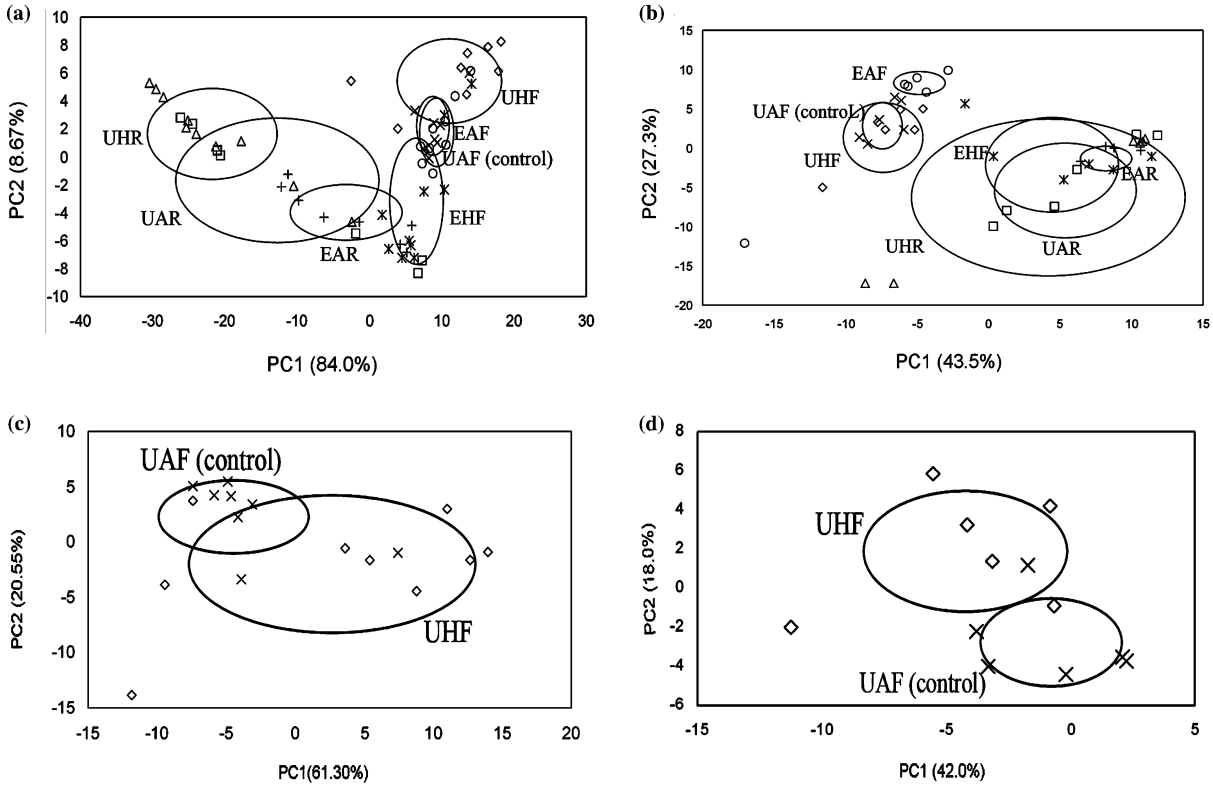

Figure 3. Principal components analyses (PCA) scores plots of (a) the entire foot muscle data set and (b) the entire digestive gland data showing the major cause of spectral variation within the data sets to be dominated by food limitation. The less significant separation observed in comparisons between unexposed fully-fed animals at elevated and ambient temperatures is displayed for (c) foot muscle, and (d) digestive gland. Symbols are: UAF (x); UHF (◇); UAR (□); UHR (△); EAF (○); EHF (✳); and EAR (+). The ellipses represent the mean + SD (along PC1 and PC2) for each of the treatment groups.

temperatures, the unexposed, elevated water temperature, reduced food (UHR) group had both higher incidence and greater severity of foot atrophy than that observed within the foot muscle of unexposed, ambient temperature, reduced food animals (UAR). In comparisons between the foot muscle of control (UAF) animals and the single stress of food reduction (UAR) we observed a 52% reduction in total NMR spectral area ($p = 0.01$), while for comparisons between increased temperature alone (UHF) versus increased temperatures along with food reduction (UHR), the foot muscle showed an 88% reduction in spectral area ($p < 0.0001$). The greater reduction of spectral areas and increased levels of foot muscle atrophy at elevated temperatures suggests a combined effect due to the presence of the two stressors.

Food limitation, however, did not cause a reduction of all foot muscle metabolites equally. One example is observed in the relationship of foot muscle glycine and carnitine. Although food reduction at 12.3 and 19 °C caused a decrease in both metabolites, we observed up to a 99% reduction in glycine levels while those of carnitine decreased much less dramatically. Glycine is utilized for numerous metabolic functions under stressful conditions, while carnitine functions as a transport molecule, modulates the coenzyme A-SH/acetyl-CoA ratio, and affects rates of the citric acid cycle as well as carbohydrate and lipid catabolism (Bremer, 1983). It is assumed that there is a greater need for carnitine where increased lipid oxidation occurs, such as during starvation. This hypothesis was verified in rats, where an increase in liver and muscle carnitine concentration upon fasting was observed (Pearson and Tubbs, 1967; Brass and Hoppel, 1978). It is likely that observed responses of individual metabolites to the stressors studied represents the preservation of key metabolites at the expense of less important ones first.

While reduced diet produced significant decreases in the total areas of foot muscle spectra, the total areas of the food-limited digestive gland spectra are preserved. This result was observed at both 19 and 12.3°C. Food reduction in the digestive gland did, however, lead to increased amounts of homarine and a peak at 2.79 ppm (possibly *N*-methyltaurine).

3.4. Metabolic response to temperature

Principal components analyses (PCAs) were performed on subsets of the data in order to evaluate the more subtle biochemical changes resulting from exposure to elevated water temperatures alone. In foot muscle, temperature alone does not result in significant

Table 1
Physical and spectroscopic parameters along with concentration ratios of selected metabolic biomarkers in both foot muscle (Ft) and digestive gland (Dg)

Treatment group	UHF		UAF (control)		UHR		UAR		EHF		EAF		EAR	
Tissue Type	Ft	Dg	Ft	Dg	Ft	Dg	Ft	Dg	Ft	Dg	Ft	Dg	Ft	Dg
NMR Total spectral Area	103 ± 16	96 ± 13	100 ± 7.5	100 ± 10	12 ± 11[a]	109 ± 49	48 ± 51[a]	119 ± 40	106 ± 8.5	155 ± 16[a]	103 ± 9.3	116 ± 5[a]	70 ± 4	140 ± 6[a]
Tissue dry/wet mass ratio (%)	29 ± 0.6[a]	35 ± 2.0	28 ± 0.6	32 ± 2.0	21 ± 2.0[a]	26 ± 3.0[a]	21 ± 0.7[a]	20 ± 4.0[a]	27 ± 2.0	29 ± 4.0	28 ± 0.6	33 ± 2.0	20 ± 2[a]	27 ± 2.0
Glucose/ homarine	0.29 ± 0.06[a]		0.18 ± 0.04		0.27 ± 0.09[a]		0.24 ± 0.23		0.13 ± 0.05[a]		0.22 ± 0.06		0.14 ± 0.03[a]	
Glycine/ homarine	12 ± 4	2.7 ± 0.2	12 ± 3	2.0 ± 0.5	0.5 ± 0.08[a]	0.85 ± 0.22[a]	0.5 ± 0.2[a]	0.7 ± 0.1[a]	2.0 ± 2.0[a]	1.0 ± 0.9	12 ± 2	2.1 ± 0.4	0.6 ± 0.1[a]	0.7 ± 0.2[a]
Osmoregulators/ amino acids	0.22 ± 0.02	0.36 ± 0.009	0.20 ± 0.02	0.35 ± 0.01	0.24 ± 0.03[a]	0.4 ± 0.04	0.21 ± 0.05	0.33 ± 0.04	0.22 ± 0.01	0.5 ± 0.13	0.22 ± 0.03	0.34 ± 0.01	0.2 ± 0.03	0.3 ± 0.1

These are selected to describe the response of the California red abalone to the various treatment groups within the experiment. Total spectral areas are normalized to control samples. All other values represent mean ± SD. Statistical significance is determined for comparisons control group (UAF).
[a]($p < 0.05$). Osmoregulators/amino acids includes (hypotaurine + glycine + betaine + homarine (digestive gland also includes *N*-methyltaurine)/all identified amino acids).

separation within the scores plots, however in the digestive gland elevated water temperatures led to significant separation along PC2 ($p < 0.05$) (figure 3c and d).

In comparisons between control (UAF) and UHF groups, elevated temperatures led to significant increases in many of the identified foot muscle metabolites. However, the total areas of foot muscle spectra were not significantly affected. Total spectral areas decreased by 12% ($p = 0.05$) in digestive gland between these same treatment groups. The high level of variance found within the food-challenged foot muscle and digestive gland spectra prevented significant differences from being detected in comparisons between UAR and UHR animals.

4. Metabolic trajectories: combined effects of food limitation and temperature

Another form of data normalization is to set the total spectral area of each NMR profile to one. Although this discards information on absolute metabolite levels (and hence the loads plots should be analyzed with caution), it provides a useful approach for comparing relative changes in metabolite levels between the treatment groups. A PCA scores plot following this type of data normalization is shown in figure 4. It is interesting to note that food limitation and temperature stress "move" the NMR spectra in opposite directions in the scores plot, indicating opposite metabolic responses to these stressors. The combination of these two stressors is probably linked through effects on metabolic rates resulting in metabolic changes in the combined food limitation and increased temperature group that is similar in nature, but greater in magnitude, than those observed under food limitation alone.

Earlier research has shown a linear relationship between temperature and oxygen consumption rate in *H. kamtschatkana* (Paul and Paul, 1998) and most published data on starvation in snails show a decrease in metabolic rates as starvation progresses (Von Brand et al., 1948; Gatty and Wilson, 1986; Carefoot, 1987). This is consistent with the trajectories that we observe along the PC1 axis, which potentially becomes an indicator of overall metabolic "fitness." Application of such methodology could be useful to the aquaculture industry allowing molecular phenotyping to serve as a tool in optimizing diets and husbandry conditions.

4.1. Metabolic response to WS-RLP infection

The presence of WS-RLP infection was observed only in animals maintained at 19°C. In this study, WS-RLP exposed abalone held at ambient water temperatures nearly failed to acquire infections (1.0% prevalence) compared to a prevalence of 72.6–93.8% of those held in heated seawater (Braid *et al.*, 2004). This,

Table 2
Relative changes in metabolite concentrations in comparisons made between various treatment groups

	Effects of starvation at_19°C (UHR vs UHF)		Effects of starvation at 12.3°C (UAR vs UAF)		Effect of elevated temperature in fully-fed abalone (UHF vs UAF)		Effect of WS-RLP infection (EHF) vs unexposed at 19°C (UHF)	
	Foot muscle	Dg	Foot muscle	Dg	Foot muscle	Dg	Foot muscle	Dg
Amino acids								
Alanine	96%↓[a]	37%↓[b]	76%↓[a]	44%↓[b]	73%↑[b]	29%↓[b]	53%↓[c]	88%↑[c]
Aspartate	87% ↓[a]	90%↑[b]	60%↓[a]	14%↑	19%↓	38%↓[c]	12%↓	50%↑
Glutamine	93%↓[a]		71%↓[a]		34%↑		44%↓[c]	
Glycine	99%↓[a]	23%↓	97%↓[a]	37%↓[b]	16%↓	14%↓	70%↓[c]	3%↓
Isoleucine	93%↓[a]	10%↑	67%↓[a]	8%↓	26%↑	29%↓[b]	30%↓	113%↑[c]
Leucine	94% ↓[a]	23%↑	75%↓[a]	13%↓	38%↑	28%↓[b]	28%↓	191%↑[c]
Lysine	97% ↓[a]	66%↑	79%↓[a]	49%↑	55%↑[b]	17%↑	54%↓[c]	45%↑
Phenylalanine	100%↓[a]		91%↓[a]		66%↑[c]		51%↓[c]	
Taurine	84% ↓[a]	18%↑	40%↓[a]	38%↑[b]	13%↓[b]	7%↓	27%↑[a]	64%↑[a]
Tryptophan	100% ↓[a]		97%↓[a]		14%↑		56%↓[b]	
Tyrosine	100%↓[a]		95%↓[a]		28%↑		53%↓[b]	
Valine	96%↓[a]	21%↑	79%↓[a]	5%↓	34%↑	31%↓[c]	56%↓[c]	165%↑[c]
Organic acids								
Formate		84%↓[a]		67%↓[b]		35%↓		84%↑
Nucleotides								
ATP/ADP	92%↓[a]	12%↓	66%↓[a]	18%↓	3%↑	2%↑	12%↓	120%↑[a]
Phosphagens								
(Phospho)Arginine	90% ↓[a]	45%↑	53%↓[a]	28%↑	10%↑	12%↓	1%↑	144%↑[a]
Carbohydrates								
α-glucose	100%↓[a]		105%↓[a]		83%↑[b]		78%↓[c]	
β-glucose	76%↓[a]		52%↓[a]		22%↑		22%↓	
Glycogen	101%↓[a]		103%↓[a]		126%↑[b]		92%↓[c]	
Organic osmolytes								
Glycine–betaine	87%↓[a]	19%↑	55%↓[a]	16%↑	nc	8%↓	9%↑	100%↑[a]
Homarine	62% ↓[a]	143%↑[c]	24%↓[a]	70%↑[c]	20%↓[b]	36%↓[a]	61%↑[a]	265%↑[a]
Hypotaurine	90% ↓[a]	70%↓[a]	34%↓[a]	30%↑	45%↑[b]	166%↑[a]	12%↓	9%↑
N-methyltaurine [d]		733%↑[c]		458%↑[a]		22%↓[b]		2187%↑[c]
Miscellaneous metabolites								
Carnitine	89%↓[a]		45%↓		9%↑		33%↑	
Acetylcholine[d]	89%↓[a]		66%↓[a]		20%↓		52%↑[b]	
Dimethyl glycine [d]		18%↓		125%↑[c]		138%↑[a]		11%↑

Arrows represent the direction of change in metabolite levels relative to non-stressed animals. Representative metabolites have been selected to illustrate the wide range of metabolite classes detectable with NMR spectroscopy. Relative metabolite levels in muscle and digestive gland tissues were calculated on a dry-mass basis. In total, 25 metabolites within the NMR spectra were quantified allowing statistical comparisons (ANOVAs) to be conducted between various treatments for these metabolite levels. Overall differences between all groups ($p < 0.001$[a], $p < 0.05$[b] $p < 0.01$[c]) with post-hoc tests revealing differences between groups.
[d]Unconfirmed assignments.

along with a high level of mortalities that occurred within the elevated water temperature, WS-RLP exposed, reduced food (EHR) group prior to the sampling date, allowed only the EHF animals to be used to assess the metabolic effects of WS-RLP infection. Interestingly, in the scores plots for both tissue types the fully fed, elevated water temperature, WS-RLP exposed (EHF) abalone lie between the fed and food-limited treatment groups. In foot muscle, elevated water temperature along with infection (EHF) separated from the single stress of elevated water temperatures (UHF; $p < 0.001$) along PC2 indicating a significant metabolic effect induced by combined WS-RLP and temperature stress. We also find that the EHF treatment separates from animals under the combined stressors of elevated temperatures and food reduction (UHR) along PC1 ($p < 0.001$). In the digestive gland EHF and UHF abalone separate along PC1 ($p < 0.0001$), however the infected group (EHF) does not significantly differ from the combined stressors of elevated temperatures and food reduction UHR.

Both the PCA scores plot and changes in individual metabolites suggest that WS-RLP infection affected the foot muscle spectrum in a less severe but similar fashion to the changes observed with food limitation. One major difference between WS-RLP infection and food limitation was an increase in foot muscle homarine levels occurring in the WS-RLP infected animals. While infection led to significant losses of both amino acids and carbohydrates, total spectral areas of the EHF foot

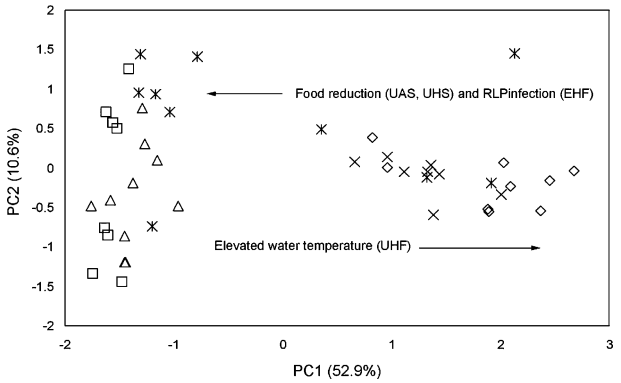

Figure 4. Foot muscle PCA scores plots with total spectral areas normalized to one facilitates visualization of the metabolic changes due to stress, along the PC1 axis. Elevated water temperatures move UHF (◇) animals to the right of control treatment group UAF (x) while starvation and infection UAR (□); UHR (△); and EHF (✳) move to the left of the control group. The ellipses represent the mean ± SD (along PC1 and PC2) for each of the treatment groups.

muscle showed no significant difference from the total spectral areas obtained from the UHF (single stress of elevated temperature) treatment.

Figure 5c shows the corresponding PCA loadings plot for the digestive gland spectra of fully-fed infected (EHF) and non-infected animals (UHF) maintained at 19°C. This plot can be used to identify which NMR peaks contribute to the differences between samples in the scores plot. For example, peaks that plot positively in the PC1 loadings plot represent metabolites that are found in higher concentrations in the samples with positive PC1 values in the corresponding scores plot. In the digestive gland WS-RLP infection led to significant increases in amino acids and osmoregulators and to a 62% increase in total spectral areas when comparing EHF and UHF treatments ($p = 0.0001$).

EHF abalone digestive glands contained significantly larger peak areas for multiple classes of metabolites than was observed in corresponding uninfected abalone. While it is unclear to what extent WS-RLP metabolites contribute to these observed changes in the digestive gland spectra, increased levels of homarine, taurine and *N*-methyltaurine (tentative assignment) also occurred in uninfected food-limited animals. In the digestive gland, the NMR data suggests that withering syndrome produces a response that is similar in many ways to the effects of starvation and which can be explained by some of the known symptoms of the disease.

4.2. Comparison of metabolic and histological measurements

Scores values for the elevated water temperature exposed (EHF) and unexposed groups (UHF) obtained from the NMR analyses of the two tissue types were evaluated against histological assessments of foot muscle degeneration, post-esophageal and digestive gland WS-RLP infection intensity, and digestive gland metaplasia and atrophy. Using digestive gland PC1 scores as a predictor in linear regression analysis we found significant relationships to exist with WS-RLP infection intensities in both post-esophageal ($r^2 = 0.91$, $p < 0.0001$) and digestive gland ($r^2 = 0.86$, $p < 0.0001$), and with digestive gland metaplasia ($r^2 = 0.6$, $p < 0.003$). Foot muscle PC2 scores showed significant relationships to both post-esophageal ($r^2 = 0.795$, $p < 0.0001$) and digestive gland WS-RLP ($r^2 = 0.63$, $p < 0.0001$) infection intensities.

4.3. Transport of metabolites between foot muscle and digestive gland

Temperature, food limitation, and WS-RLP infection had a less significant effect on abalone digestive gland than foot muscle, and in many cases the metabolite changes within the two tissues occurred in the opposite directions. This suggests that foot muscle serves as a storage organ with transport likely occurring to the digestive gland. Observations in the current study suggest that abalone catabolize foot muscle metabolites in order to maintain metabolic demands while preserving the integrity of the digestive gland. Histological observations once again are consistent with this finding; starvation did not cause a significant increase in digestive gland atrophy in comparisons made between the digestive glands of unexposed fed and unexposed starved animals. In abalone, unlike many other animals, the digestive gland, and not intestine, performs nutrient absorption. Thus a fully functional digestive gland is crucial for maintaining homeostasis and survival (Voltzow, 1994).

Within the current study, taurine decreased by 40% ($p = 0.001$) in foot muscle due to food limitation alone; however, it increased by 38% ($p = 0.05$) in the digestive gland. This has been previously observed in *H. diversicolor*, where taurine and crude protein in foot muscle decreased while concurrently increasing in viscera (Chiou *et al.*, 2001). Food reduction at both temperatures resulted in similar trends in homarine levels. It has also been observed that total lipid in the foot muscle of *H. fulgens* fed *Egresia menziesii* decreased between spring and fall, while at the same time levels increased in the digestive gland and gonad (Nelson *et al.*, 2002). Metabolite trafficking has also been documented in crayfish (*Procambarus clarkii*) where L-Ala was observed to be transported from the muscle to the digestive gland (Okama and Abe, 1998).

4.4. Changes in free amino acids

In foot muscle spectra, WS-RLP infection and food reduction at both elevated and ambient temperatures led to a decrease in free amino acids, organic osmolytes and carbohydrates. During starvation, free amino acids must

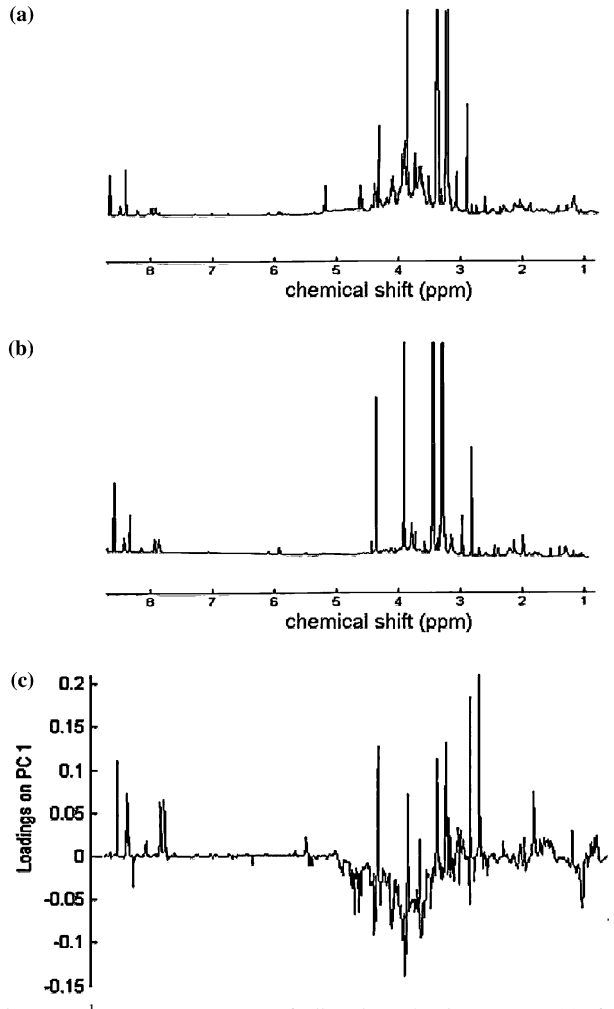

Figure 5. ^{1}H NMR spectra of digestive gland extracts: (a) fed, uninfected abalone in 19 °C seawater (UHF), (b) fed, WS-RLP infected abalone in 19 °C seawater (EHF), and (c) PCA loadings plot representing the metabolic differences between these two treatment groups.

be produced by structural protein hydrolysis (Okama and Abe, 1998). While it has generally been considered that the main role of free amino acids is in osmoregulation (Dall, 1975; Schoffeniels, 1976; McCoid *et al.*, 1984), abalone, as with other marine invertebrates, will also depend on this pool as an energy source during periods of prolonged starvation (McCoid *et al.*, 1984). This is most likely causing the observed decrease in foot muscle amino acids in WS-RLP infected and food challenged animals. Thus, as levels of free amino acids are depleted, osmoregulation is maintained by increased concentrations of less metabolically active compounds. Such compounds include non-essential amino acids such as betaines, the nitrogenous base trimethylamine oxide, and other compounds dependent upon species (Riley, 1976).

Within each treatment group the peak areas of taurine and glycine–betaine consistently produced the two largest NMR peaks in both tissues. Free amino acid measurements made in *H. rufescens* (Allen and Kilgore, 1975), *H. discus* (Hatae *et al.*, 1995), and *H. diversicolor* (Hwang *et al.*, 1997) all found taurine to be the most abundant free amino acid present in abalone tissue. While food limitation caused reductions in all of the identified foot muscle metabolites, taurine and glycine–betaine continued to produce the largest NMR peaks. Taurine, a secondary amino acid, is an important intracellular osmoregulator in a number of marine invertebrates (Kasschau, 1975), and glycine–betaine is an energetically expensive molecule to synthesize, requiring the reductive assimilation of nitrate and several subsequent methylations. It is therefore likely that the maintenance and synthesis of important and energetically costly compounds will be under strict control within the cells (Keller *et al.*, 1999).

4.5. Application of the glucose/homarine ratio

Homarine, an endogenously synthesized heteroaromatic quaternary ammonium compound, was found to be elevated in hemolymph, foot muscle and digestive gland samples from WS-RLP infected red abalone (Viant *et al.*, 2003). It is found almost exclusively in marine organisms, and is believed to serve in osmoregulation as well as a transmethylating agent (Netherton and Gurin, 1982). It may also possess morphogenetic activity, affecting pattern formation, cell differentiation and cell proliferation within *Hydractinia* tissue (Berking, 1987). While it is quite likely that increased homarine levels buffer osmoregulation, its morphogenetic activity possibly plays a role in the association that exists between WS-RLP infection and the observed metaplasia that occurs within the digestive glands of infected animals (Gardner *et al.*, 1995). In earlier studies, *increased* levels of homarine in abalone tissue with WS (Viant *et al.*, 2003), along with reported *decreased* levels in foot muscle of starved disk abalone (Watanabe *et al.*, 1993), led to the idea that homarine could act as a discriminatory biomarker of WS versus starvation (Viant *et al.*, 2003). Glucose levels, which decrease in stressed abalone (Carefoot *et al.*, 1993), were evaluated against levels of homarine producing a glucose/homarine ratio.

In hemolymph samples taken from the current study, it was found that food deprived and WS-RLP infected abalone produced glucose/homarine ratios that were statistically equivalent and were both significantly smaller than those obtained from control animals (control, 1.98 ± 0.9; food deprived, 0.33 ± 0.24; and WS-RLP infected, 0.99 ± 0.76; Viant *et al.*, 2003). In both foot muscle and digestive gland, we observe increased levels of homarine with WS-RLP infection. However, food reduction resulted in decreased levels of homarine in foot muscle only (table 2). Thus with the use of the glucose/homarine ratio in foot muscle, rather than hemolymph, we find significant increases occurring in both the unexposed fed and food limited groups at elevated temperatures and significant decreases in both the exposed heated fed and the exposed ambient reduced food groups (table 1).

The conclusion that the glucose/homarine ratio increases in food limited foot muscle and decreases in WS-RLP foot muscle is somewhat confounded both by the response of this biomarker in the WS-RLP exposed groups at ambient temperatures. While histologically both these groups of animals appeared uninfected the amount of tissue available for histology was quite small, possibly allowing light WS-RLP infections to have been missed (Braid *et al*., 2004). These same histological examinations found body shrinkage and foot degeneration to be highly correlated within treatment groups known to host WS-RLP infection. While no correlation between foot degeneration and body shrinkage was observed in either uninfected food limited groups or in the EAF animals, it was correlated in the EAR animals (Braid, personal communication). Within the EAR group, both the homarine levels and glucose/homarine ratios were similar to those of abalone with known WS-RLP infection. It is possible that glucose/homarine values initially decrease due to the short-term response of glucose to food reduction and then begin to increase in late stage starvation due to the depletion of secondary metabolites such as homarine. It is perhaps more likely that the glucose/homarine ratio reflects the presence of WS-RLP infections that have not been detected by histology. Evaluation of the glucose/homarine ratio along a time course of starvation and WS pathogenesis however is required before this ratio can definitively be used to distinguish WS-RLP infected animals from both control and food limited groups.

5. Concluding remarks

Results from this study suggest that further investigations are needed before the recently established glucose/homarine ratio can be used to definitively separate California red abalone with known WS-RLP infections from that of both healthy and food limited abalone. Furthermore, we have illustrated a robust correlation between the NMR metabolic data with traditional histological measurements, the established "gold standard" for disease diagnosis. These conclusions strongly support the further development and integration of metabolomics as a complementary tool for identifying and characterizing pathological events in aquatic species, particularly during periods of environmentally relevant stress. In the current study, we found that food limitation in conjunction with elevated temperatures resulted in the greatest reduction of foot muscle metabolites. This observation suggests that thermally modulated basal metabolic rates, along with decreased food availability, act in an additive manner, leading to a more rapid depletion of foot muscle metabolites. It was also clear that the severity of changes in foot muscle due to food limitation is greater than the perturbations caused by WS-RLP infection. This suggests that animals infected with WS-RLP do not immediately lose the ability to use external food sources and that the loss of appetite previously observed in animals experiencing WS (Moore *et al*., 2000, 2001) occurs only in the later stages of the disease.

Acknowledgments

Support was provided in part by the National Sea Grant College Program of the U.S. Department of Commerce's National Oceanic and Atmospheric Administration under NOAA Grant #NA06RG0142, project R/A-117. We thank T. Robbins, J.S. de Ropp, and J.E. Murphree for technical assistance. MRV is indebted to the Natural Environment Research Council, UK, for the award of an Advanced Fellowship (NER/J/S/2002/00618).

References

Allen, W.V. and Kilgore, J. (1975). The essential amino acid requirements of the red abalone, *Haliotis rufescens*. *Comp. Biochem. Physiol.* **50**, 771–775.

Andree, K.B., Friedman, C.S., Moore, J.D. and Hedrick, R.P. (2000). A polymerase chain reaction assay for the detection of genomic DNA of a Rickettsiales-like prokaryote associated with withering syndrome in California abalone. *J. Shellfish Res.* **19**, 213–218.

Bayne, B.L. (1985). The effects of stress and pollution on marine animals in Bayne, B.L., Brown, D.A. and Burns, K., *et al*. (Eds), *Ecological Consequences of Stress*. Praeger, New York, pp. 141–157.

Berking, S. (1987). Homarine (*n*-methylpicolinic acid) and trigonelline (*N*-methylnicotinic acid) appear to be involved in pattern control in a marine hydroid. *Development* **99**, 211–220.

Braid, B.A., Moore, J.D., Robbins, T.T., *et al*. (2004). Biochemical and histologic changes in red abalone (*Haliotis rufescens*) subjected to eight different treatment combinations of exposure to the agent of withering syndrome, water temperature, and food availability. MS Thesis, UC Davis, 1–98.

Brass, E.P. and Hoppel, C.L. (1978). Carnitinte metabolism in the fasting rat. *J. Biol. Chem.* **253**, 2688–2693.

Bremer, J. (1983). Carnitinte Metabolism and functions. *Physiol. Rev.* **63**, 1420–1480.

Carefoot, T.H. (1987). Diet and its effect on oxygen uptake in the sea hare Aplysia. *J. Exp. Mar. Biol. Ecol.* **114**, 275–287.

Carefoot, T.H., Qian, P.Y., Taylor, B.E., West, T. and Osborne, J. (1993). The effects of starvation on energy reserves and metabolism in the northern abalone, *Haliotis kamtschatkana*. *Aquaculture* **118**, 315–325.

Chiou, T., Lai, M. and Shiau, C. (2001). Seasonal variations of chemical constituents in the muscle and viscera of small abalone fed different diets. *Fish. Sci.* **67**, 146–156.

Dall, W. (1975). The role of ninhydrin-positive substances in osmoregulation in the western rock lobster, *Panulirus longipes*. *J. Exp. Mar. Biol. Ecol.* **19**, 43–58.

Fan, T. (1996). Metabolite profiling by one and two dimensional NMR analysis of complex mixtures. *Prog. Nucl. Magn. Reson.* **28**, 161–219.

Friedman, C.S., Andree, K.B., Robbins, T.T., *et al*. (2000). "*Candidatus Xenohaliotis californiensis*," a newly described bacterial pathogen and etiological agent of withering syndrome found in abalone *Haliotis* spp., along the west coast of North America. *J. Shellfish Res.* **19**, 513.

Friedman, C.S. and Finley, C.A. (2003). Anthropogenic introduction of the etiological agent of withering syndrome into northern California abalone populations via conservation efforts. *Can. J. Fish. Aquat. Sci.* **60**, 1424–1431.

Friedman, C.S., Thomson, M., Chun, C., *et al.* (1997). Withering syndrome of the black abalone *Haliotis cracherodii* (Leach): Water temperature, food availability, and parasites as possible causes. *J. Shellfish Res.* **16**, 403–411.

Gardner, G.R., Harshbarger, J.C., Lake, J., *et al.* (1995). Association of prokaryotes with symptomatic appearance of withering syndrome in black abalone *Haliotis cracherodii*. *J. Invertebr. Pathol.* **66**, 111–120.

Gatty, G. and Wilson, J.H. (1986). Effect of body size starvation, temperature and oxygen tension on the oxygen consumption of hatchery reared ormers *Haliotis tuberculata* L. *Aquaculture* **56**, 229–237.

Hwang, D., Liang, W., Shiau, C., Chiou, T. and Jeng, S. (1997). Seasonal variations of free amino acids in the muscle and viscera of small abalone *Haliotis diversicolor*. *Fish. Sci.* **63**, 625–629.

Hatae, K., Nakai, H., Shimada, A., *et al.* (1995). Abalone (*Haliotis discus*): seasonal variations in chemical composition and textural properties. *J. Food Sci.* **60**, 32–35.

Isani, G., Serra, R., Cattani, O., Cortesi, P. and Carpene, E. (1997). Adenylaye energy charge and metallothionein as stress indices in Mytilus galloprovincialis exposed to cadmium and anoxia. *J. Mar. Biol. Assoc. UK* **77**, 1187–1197.

Kasschau, M.R. (1975). The relationship of free amino acids to salinity changes and temperature-salinity interactions in the mud flat snail, *Nassarius obsoletus*. *Comp. Biochem. Physiol.* **51**, 301–308.

Keller, M.D., Kiene, R.P., Matrai, P.A and Bellows, W.K. (1999). Production of glycine betaine and dimethylsulfoniopropionate in marine phytoplankton. II. N-limited chemostat cultures. *Mar. Biol.* **135**, 249–257.

Kismohandaka, G., Friedman, C.S., Roberts, W., Hedrick, R.P. and Crosby, M.P. (1993). Investigation of physiological parameters of black abalone with withering syndrome. *J. Shellfish Res.* **12**, 131–132.

Lafferty, K.D. and Kuris, A.M. (1993). Mass mortality of abalone *Haliotis cracherodii* in the California Channel Islands: tests of epidemiological hypotheses. *Mar. Ecol. Prog. Ser.* **96**, 239–248.

McCoid, M., Miget, R. and Finne, G. (1984). Effect of environmental salinity on the free amino acid compostion and concentration in penaeid shrimp. *J. Food Sci.* **49**, 327–330.

Moore, J.D., Robbins, T.T. and Friedman, C.S. (2000). Withering syndrome in farmed red abalone, *Haliotis rufescens*: thermal induction and association with a gastrointestinal Rickettsiales-like prokaryote. *J. Aquat. Animal Health* **12**, 26–34.

Moore, J.D., Robbins, T.T., Hedrick, R.P. and Friedman, C.S. (2001). Transmission of the rickettsiales-like prokaryote *Candidates Xenohalliotis californiensis* and its role in withering syndrome of California abalone. *J. Shellfish Res.* **20**, 867–874.

Moore, J.D., Finley, C.A., Robbins, T.T. and Friedman, C.S. (2002). Withering syndrome and restoration of Southern California abalone populations. *California Coop. Ocean. Fish. Invest. Rep.* **43**, 112–117.

Nelson, M.W., Leighton, D.L., Phleger, C.F. and Nichols, P.D. (2002). Comparsion of the growth and lipid compostion in the green abalone *Haliotis fulgens*, provided specific macroalgal diets. *Comp. Biochem. Physiol. Part B* **131**, 695–712.

Netherton, J.C. and Gurin, S. (1982). Biosynthesis and physiological role of homarine in marine shrimp. *J. Biol. Chem.* **257**, 11971–11975.

Okama, E. and Abe, H. (1998). Effects of starvation and D-or L-alanine administration on the free D- and L-alanine levels in the muscle and hepatopancrease of the crayfish *Procambarus clarkia*. *Comp. Biochem. Physiol. Part A* **120**, 681–686.

Paul, A.J. and Paul, J.M. (1998). Respiration rate and thermal tolerances of pinto abalone *Haliotis kamtschatkana*. *J. Shellfish Res.* **17**, 743–745.

Pearson, D.J. and Tubbs, P.K. (1967). and derivatives in rat tissues. *Biochem. J.* **105**, 953–963.

Rainbow, P.H. and Phillips, D.J.H. (1993). Cosmopolitan biomonitors of trace metals. *Mar. Poll. Bull.* **26**, 593–601.

Raimondi, P.T., Wilson, C.M., Ambrose, R.F., *et al.* (2002). Continued declines of black abalone along the coast of California: are mass mortalities related to El Nino events? *Mar. Ecol. Prog. Ser.* **242**, 143–152.

Riley, R.T. (1976). Changes in the total protein, lipid, carbohydrate, and extracellular body fluid free amino acids of the pacific oyster, *Crassostrea gigas*, during starvation. *Proc. Nat. Shellfish Assoc.* **65**, 84–90.

Schoffeniels, E. (1976). Adaptation with respect to salinity. *Biochem. Soc. Symp.* **41**, 179–204.

Shields, J.D., Perkins, F.O. and Friedman, C.S. (1996). Hematological pathology of withering syndrome. *J. Shellfish Res.* **15**, 498.

Viant, M.R. (2003). Improved methods for the acquisition and interpretation of NMR metabolomic data. *Biochem. Biophys. Res. Comm.* **310**, 943–948.

Viant, M.R, Rosenblum, E.S. and Tjeerdema, R.T. (2003). NMR-based metabolomics: a powerful approach for characterizing the effects of environmental stressors on organism health. *Environ. Sci. Technol.* **37**, 4982–4989.

Vilchis, L.I., Tegner, M.J., Moore, J.D., Friedman, C.S., *et al.* (2005). Effects of ocean warming on the growth, reproduction, and survivorship of red and green abalones in southern California: implications for restoration and recovery of depleted stocks. *Ecol. Appl.* **15**, 469–480.

Voltzow, J. (1994). Gastropoda: Prosobranchia in Harrison, F. and Humes, A. (Eds), *Microscopic Anatomy of Invertebrates, Vol. 3*. Wiley-Liss Publishers, New York, pp. 11–252.

Von Brand, T., Nolan, M.O. and Mann, E.R. (1948). Observations on the respiration of Australorbis glabratus and some other aquatic snails. *Biol. Bull. Woods Hole.* **95**, 199–213.

Watanabe, H., Yamanaka, H. and Yamakawa, H. (1993). Changes in the content of extractive components in disk abalone fed with marine algae and starved. *Nippon Suisan Gakk.* **59**, 2031–2036.